Ocean Engineering 266 (2022) 112803

Contents lists available at ScienceDirect

Ocean Engineering

journal homepage: www.elsevier.com/locate/oceaneng

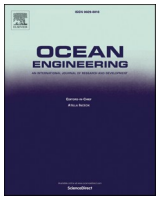

Assessment of the use of scatterometer wind data to force wave models in the North Atlantic Ocean

Dina Silva [a], Marta Gonçalves [a], Abderrahim Bentamy [b], C. Guedes Soares [a,*]

[a] Centre for Marine Technology and Ocean Engineering (CENTEC), Instituto Superior Técnico, Universidade de Lisboa, Av. Rovisco Pais, 1049-001, Lisboa, Portugal
[b] Laboratoire Spatial et Interfaces Air-Mer (IFREMER), Centre Bretagne - ZI de la Pointe du Diable, CS 10070, 29280, Plouzané, France

ARTICLE INFO

Keywords:
ERA-Interim
ERA5
Satellite
Azores
Madeira

ABSTRACT

The present work uses for the first time scatterometer wind fields to force a wave model and compares the accuracy of the resulting wave conditions with the ones obtained when using two different sources of hindcast wind fields forcing the same wave spectral model in the Atlantic Ocean. For this purpose, a 5-year hindcast (2010–2014) is performed with the wave spectral model SWAN for the Madeira and Azores archipelagos. The model uses as input the bathymetry from GEBCO, the wave boundary conditions from the WAVEWATCH III wave model provided by Ifremer and winds from the ERA-Interim and ERA5 databases, and remotely sensed winds from scatterometers. A quantitative analysis of the results is performed, and the numerical results are validated against altimeter data and buoy measurements. Globally, ERA-Interim, ERA5 and scatterometer wind data provided similar accuracy of the generated wave fields, as expressed in the error statistics, which are very close to each other, but in the case of extreme events, the scatterometer data reveals more intense winds and consequently lead to sea states with higher significant wave height. This is more visible in the Azores area than in Madeira. The results demonstrate that, in general, the significant wave height is well reproduced by SWAN.

1. Introduction

Characterizing the wave climate with accuracy is of great importance for different purposes, like maritime transportation, ocean and civil engineering. This knowledge helps to study the responses of the maritime structures to the wave forcing, assisting the appropriate design of the vessels and devices according to where they will be operated.

The early measurements of sea state conditions relied on in situ measurements, mostly by waverider buoys, which have been gradually supplemented by remotely sensed information such as altimetry or SAR (Synthetic Aperture Radar). The wave's buoys networks around the world are scattered and limited in terms of spatial coverage, since they only give measurements in situ, and are mostly relatively close to the coasts. Satellite data can fill this gap by providing data across the ocean, in an evenly distributed fashion.

Satellite data started being used with wave data determined from altimeters and have progressed to more sophisticated tools, such as SAR (Synthetic Aperture Radar) data and moved later from measurements of wave conditions to wind measurements with scatterometers and radiometers (Bentamy et al., 2002).

Nowadays, the numerical wave spectral models are widely accepted to determine the sea states, in response to wind forcing, and can be used to hindcast, nowcast and forecast (Cavaleri et al., 2007; Mulligan et al., 2011; Roland and Ardhuin, 2014; Stopa et al., 2016; Campos et al., 2022). The third-generation spectral wave models are currently used to account for wave generation in deep waters, such as WAM (WAve model) (WAMDI Group, 1988) and WWIII (WAVEWATCHIII) (Tolman, 1991), and wave propagation in coastal areas, such as SWAN (Simulating WAves Nearshore) (Booij et al., 1999). The WWIII and WAM models solve the equation of wave spectrum using explicit propagation schemes in geographical and spectral spaces, which in shallow water requires very small grid sizes and this is inconvenient for coastal regions applications. SWAN use implicit schemes, which are more robust and economic in shallow water. However, the newest versions of WWIII are also suitable for shallow waters with an improvement of the numerical approach with an implicit scheme.

It is possible to nest one model representing the waves in deep water with another one simulating the waves in the nearshore, taking into account the evolution of the wave spectrum from the generation until their transformation in shallow waters. There are several applications of this procedure for example in Guedes Soares et al. (2011).

The wind fields are an important input for the wave models since the

* Corresponding author.
E-mail address: c.guedes.soares@centec.tecnico.ulisboa.pt (C. Guedes Soares).

https://doi.org/10.1016/j.oceaneng.2022.112803
Received 11 May 2021; Received in revised form 19 September 2022; Accepted 2 October 2022
Available online 17 October 2022

Table 1
Characteristics of the ERA5 and ERA-Interim reanalyses.

Characteristics	ERA-Interim	ERA5
Implementation date	12 Dec 2006	8 Mar 2016
Horizontal resolution	~79 km	~31 km
Horizontal transform grid	0.75°x0.75 °	0.3°x 0.3 °
Vertical resolution	60 levels up to 0.1 hPa	137 levels up to 0.01 hPa
Temporal resolution	6-hourly	Hourly
IFS cycle	31r2	41r2
Period covered	1979–August/2019	1950–now

Table 2
Websites with information about radars and radiometers used in this study.

Satellite	Period	Website
ASCAT	2006 – Present	projects.knmi.nl/scatterometer/ascat_osi_12_prod
SSMI/S F16	2003 - Present	http://data.remss.com/ssmi/f16/bmaps_v07/
SSMI/S F17	2007 - Present	http://data.remss.com/ssmi/f17/bmaps_v07/
WindSat	2003 - Present	http://data.remss.com/windsat/bmaps_v07.0.1/
Sentinel SAR	2014 - Present	https://sentinel.esa.int/web/sentinel/missions/sentinel-1/data-products

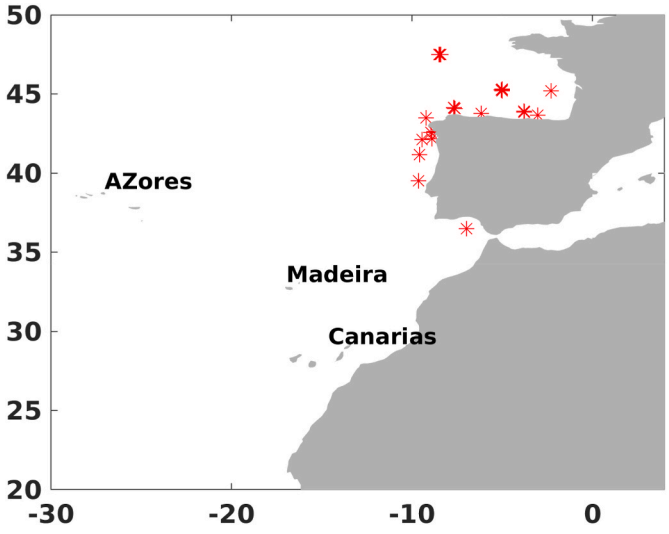

Fig. 1. Buoys used for the determination of satellite wind analysis accuracy. Their locations are shown as star symbols.

Table 3
Numeric parameters for the WWIII Ifremer Global grid.

Parameter	Coarse Grid
Temporal resolution	3h
Spatial resolution	0.5° (30min)
Frequencies	32
Frequency domain	0.037–0.72Hz
Directional band	24
Latitudes	80°N –78°S
Longitudes	180°W – 179.5°E
Wind Forcing	ERA 5
Wind input time step	3h

waves are generated by the transfer of wind energy to the ocean surface, and their accuracy will reflect significantly in the resulting sea states (Teixeira et al., 1995; Holthuijsen et al., 1996; Cavaleri and Bertotti, 2006; Ponce de León and Guedes Soares, 2008). Nowadays there are a

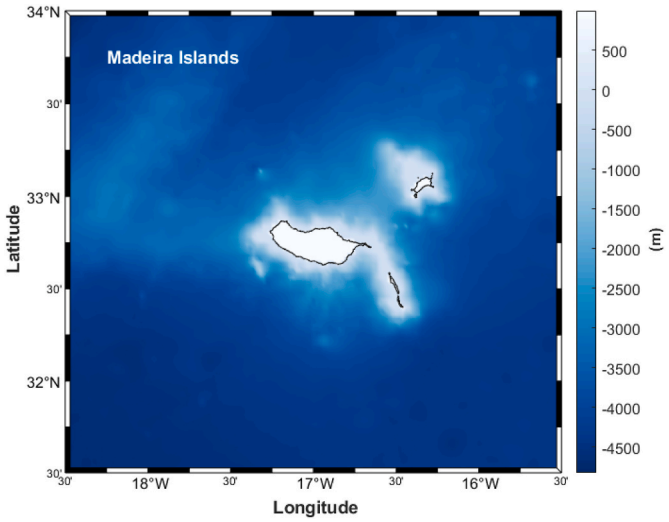

Fig. 2. Bathymetry of Madeira grid area.

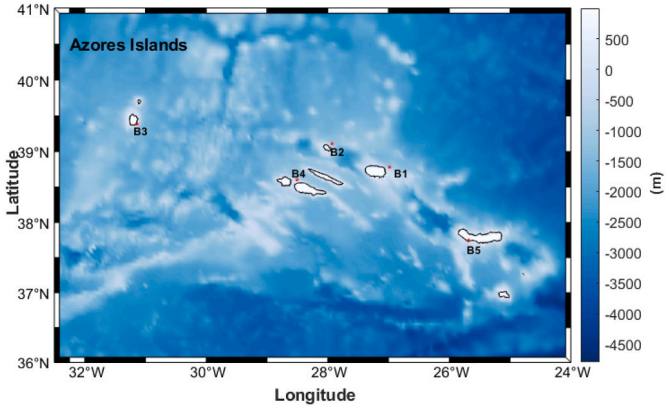

Fig. 3. Bathymetry of Azores grid area and positions of buoys.

Table 4
Hindcast system grid information.

	Latitude/Longitude	Resolution
Azores	36°N to 41°N/32.5°W to 24°W	0.05° × 0.05°
Madeira	31.5°N 34°N/18.5°W to 15.5°W	0.02° × 0.02°

Table 5
Locations of Azores Buoys.

Buoy	Latitude	Longitude	Depth (m)
Praia Vitoria (B1)	38° 45.05′N	27° 00.62′W	100m
Graciosa (B2)	39° 05.21′N	27° 57.73′W	97m
Lages (B3)	39° 22.11′N	31° 09.80′W	80m
Faial/Pico (B4)	38° 35.26′N	28° 32.26′W	110m
Ponta Delgada (B5)	37° 43.53′N	25° 43.28′W	90m

considerable number of wind data provided by a variety of international organizations, such as ECMWF (European Centre for Medium-range Weather Forecast, https://www.ecmwf.int/), and NCEP (National Centers for Environmental Predictions, https://psl.noaa.gov/data/gridded/data.ncep.reanalysis.html), Copernicus (https://cds.climate.copernicus.eu/) that produce datasets with different temporal and spatial resolutions, as discussed by Campos and Guedes Soares (2017).

Several studies were performed comparing these different reanalyses datasets available. Stopa and Cheung (2014) described an

Table 6
Statistical results for Hs for Azores Islands.

Wind Forcing	Buoy	BIAS	RMSE	SI	r	# points
ERA-Interim	**B1**	−0.08	0.47	0.30	0.86	3486
	B2	−0.21	0.62	0.34	0.80	11418
	B3	−0.07	0.43	0.25	0.89	7563
	B4	0.28	0.51	0.31	0.89	13944
	B5	0.01	0.39	0.29	0.87	9377
ERA-5	**B1**	−0.08	0.47	0.30	0.86	3486
	B2	−0.19	0.60	0.34	0.78	11418
	B3	−0.07	0.40	0.24	0.90	7563
	B4	0.28	0.51	0.31	0.89	13944
	B5	0.04	0.39	0.29	0.88	9377
Satellite	**B1**	−0.06	0.45	0.29	0.87	3486
	B2	−0.20	0.60	0.33	0.81	11418
	B3	−0.03	0.40	0.24	0.90	7563
	B4	0.29	0.51	0.31	0.89	13944
	B5	0.03	0.39	0.30	0.87	9377

intercomparison of wind and wave heights from ERA-Interim (Dee et al., 2011) and CFSR (Saha et al., 2010). The errors for these datasets are comparable, with an improvement of these products related to their predecessors R1 (NCEP global Reanalysis I) and ERA-40, with consistent levels of accuracy for significant wave height and wind speed in the Northern and Southern Hemispheres.

Campos and Guedes Soares (2016a) have produced a comparison between hindcast winds and between hindcast waves in the North Atlantic Ocean, considering two different reanalysis datasets: HIPOCAS (Guedes Soares, 2008) and ERA reanalysis. The study shows that HIPOCAS tends to overestimate the wind measurements from satellites while both ERA reanalysis (ERA-40 and ERA-Interim) tend to underestimate them. A comparison between ERA-Interim, NOAA/CFSR and HIPOCAS was made by Campos and Guedes Soares (2016b), showing that for the general non-extreme conditions (calm and moderate weather), the three wave hindcasts are very similar, but under extreme conditions, significant differences of significant wave heights were found among hindcasts at latitudes above 40° north.

Lavidas et al. (2017) studied the sensitivity of the numerical wave model SWAN on wind reanalysis datasets. The study focused on ERA-Interim (ECMWF) and the CFSR (NCEP) reanalysis datasets and shows that for the western coastline of Scotland, the ERA-Interim outperforms CFSR hindcasting the wave resource, with smaller biases, low RMS (Root Mean error) which is a measure of the differences between measurements and simulated values, and less scattering.

In Rusu et al. (2018), a wave prediction system was set up to predict storm conditions on the Western Iberian coast. Two spectral wave models (WAM and SWAN), and two different wind reanalysis datasets (ERA-Interim and CFSR) were used. The results show that under extreme wave conditions both simulations demonstrate a reasonable accuracy in the predictions, nevertheless, some underestimations of the peak events were observed.

Among the diversity of methods available to study wind resources, from onsite measurements, reanalysis datasets, satellite data or numerical prediction models, remote sensing information is frequently used due to the high spatial and temporal resolutions provided in the estimations of the surface wind vectors (Jiang et al., 2013; Bentamy and Croize-Fillon, 2014).

Surface winds from scatterometer missions have been used to produce climate series (Ricciardulli and Manaster, 2021; Verhoef et al., 2016). Several studies have been made on the quality of the scatterometer products (Verspeek et al., 2010; Bentamy et al., 2008; Sudha and Prasada Rao, 2013), proving that remotely sensed winds are statistically in agreement with in situ measurements.

Given the nature of the scatterometer wind data and its quality, this work aims at comparing the wave hindcasts that use scatterometer data as the wind input with the ones that are forced with established hindcast wind fields, such as ERA-Interim and ERA5 reanalysis. These winds force the SWAN wave model applied to the Portuguese Atlantic islands of the Azores and Madeira, which have been chosen because they represent wave conditions well in the North Atlantic. In addition, the context of islands usually has a more complicated wave propagation due to the sheltering effect of other islands, which can induce big changes in the wave field, Ponce de León and Guedes Soares (2005, 2010), and Gonçalves et al. (2020).

The target areas have been studied earlier by Rusu et al. (2008), Rusu and Guedes Soares (2012), Silva et al. (2018), Silva and Guedes Soares (2021a, 2021b), Gonçalves and Guedes Soares (2021a, 2021b).

2. Description of datasets

2.1. ERA-Interim

ERA-Interim (Dee et al., 2011) is a global atmospheric reanalysis of

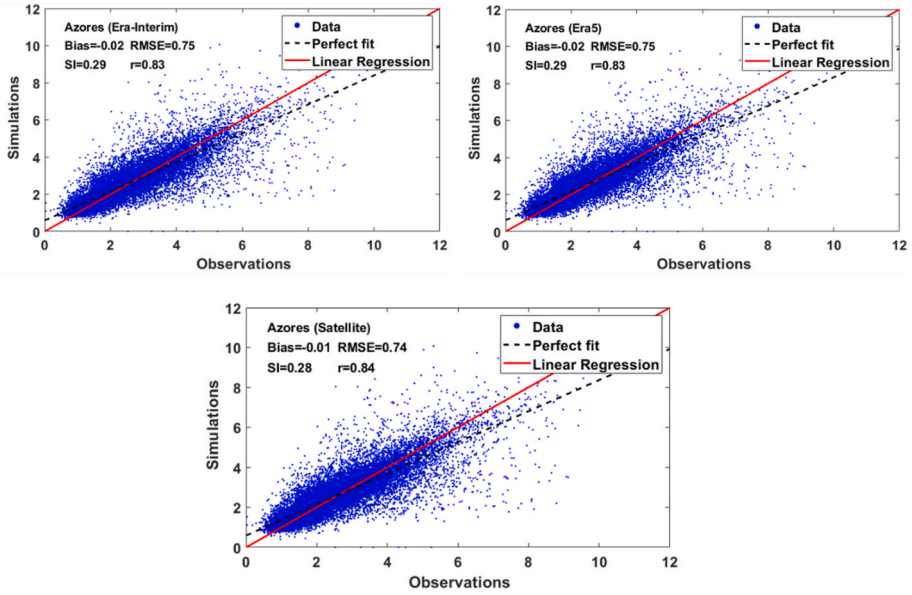

Fig. 4. Scatter index for all hindcasts against satellite data for the Azores between the period 2010–2014.

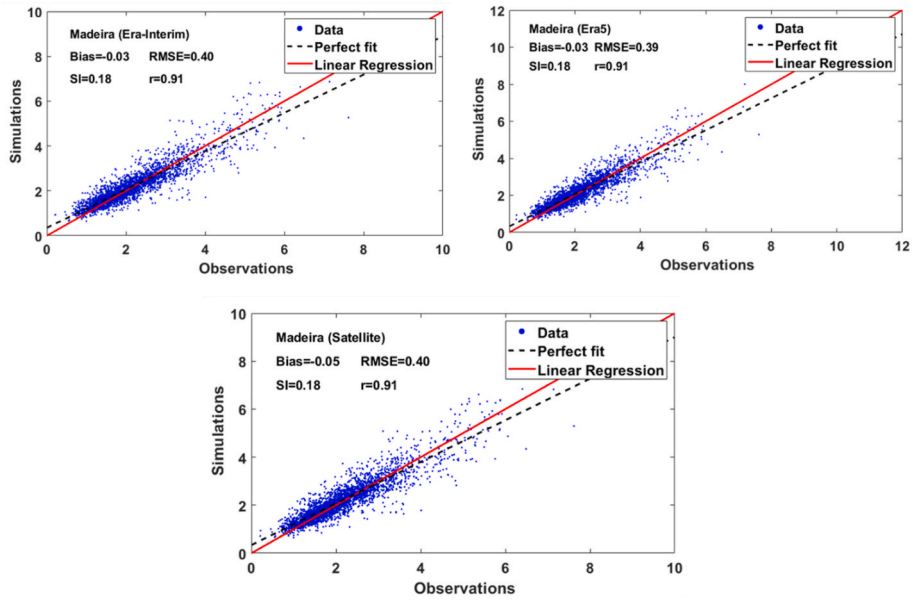

Fig. 5. Scatter index for all hindcasts against satellite data for Madeira between the period 2010–2014.

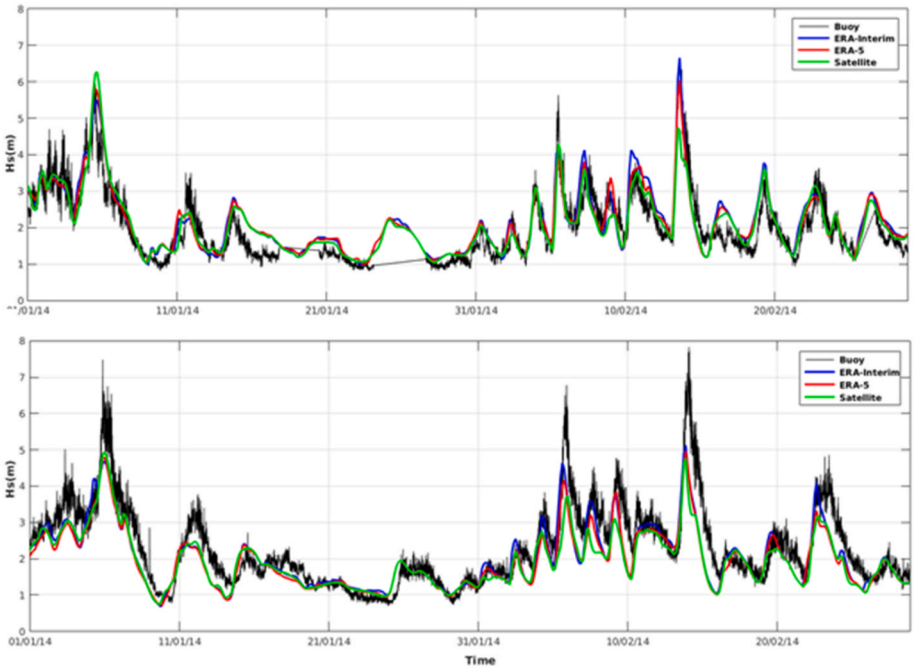

Fig. 6. Time series of the significant wave height for the Azores. B3 buoy (on top) and B5 buoy (on the bottom) as simulated by SWAN using ERA-Interim (blue line), ERA-5 (red line) and Satellite wind (green line) against measured data from buoys (black line). (For interpretation of the references to colour in this figure legend, the reader is referred to the Web version of this article.)

data from 1979 up to August 2019, using ECMWF's Integrated Forecast System (IFS) cycle 31r2, released in 2006, with ~79 km of horizontal resolution on 60 model levels from the surface up to 0.1 hPa (an altitude of about 65 km).

When compared with its previous reanalysis (such as ERA40) ERA-Interim presents a better performance, better data assimilation methods, finer resolution and an improved physics of the models as described in (Dee et al., 2011). ERA-Interim also includes data assimilation from satellites for the wave results starting in 1991, as the European Remote Sensing Satellites 1 and 2 (ER1 and ER2), Environmental Satellite (ENVISAT), JASON-1, and JASON-2. The ERA-Interim products resolution is approximately 0.70° × 0.70° and 3h, case of wind, and 0.64° × 0.64° and 6h, case of waves.

2.2. ERA-5

As part of implementing the EU-funded Copernicus Climate Change Service (C3S), ERA5 (Hersbach and Dee, 2016) is global weather and climate reanalysis, produced by the ECMWF from January 1950 to the present, replacing the ERA-Interim reanalysis. ERA5 is based on 4D-Var data assimilation using Cycle 41r2 of the Integrated Forecasting System (IFS), which was operational at ECMWF in 2016. Benefiting from a decade of advances in model physics, core dynamics and data assimilation relative to ERA-Interim, ERA5 presents a significantly enhanced

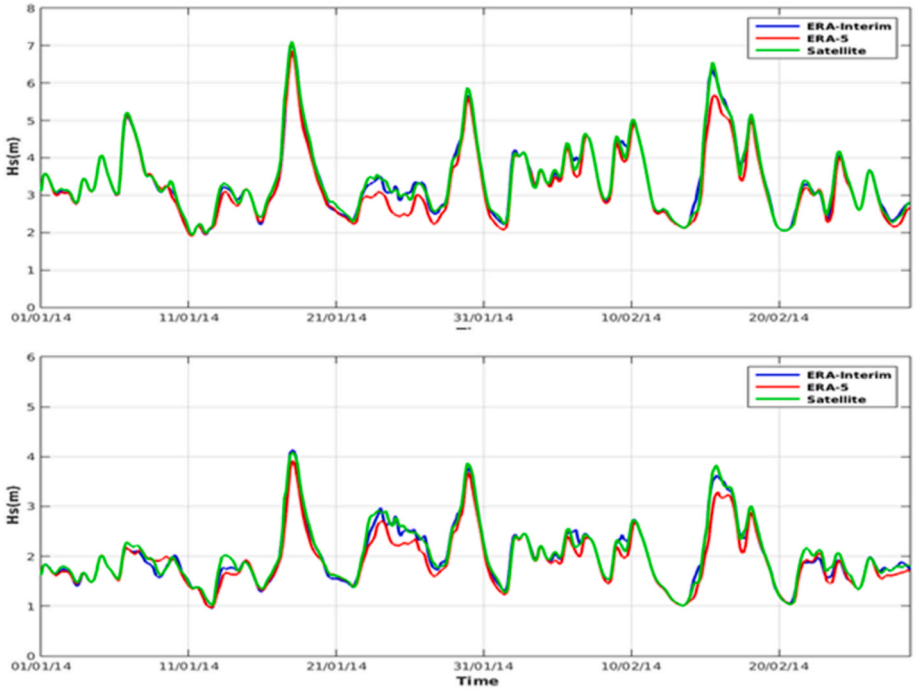

Fig. 7. Time series of the significant wave height for Madeira. São Vicente buoy (on top) and Caniçal buoy (on the bottom) locations as simulated by SWAN using ERA-Interim (blue line), ERA-5 (red line) and Satellite wind (green line). (For interpretation of the references to colour in this figure legend, the reader is referred to the Web version of this article.)

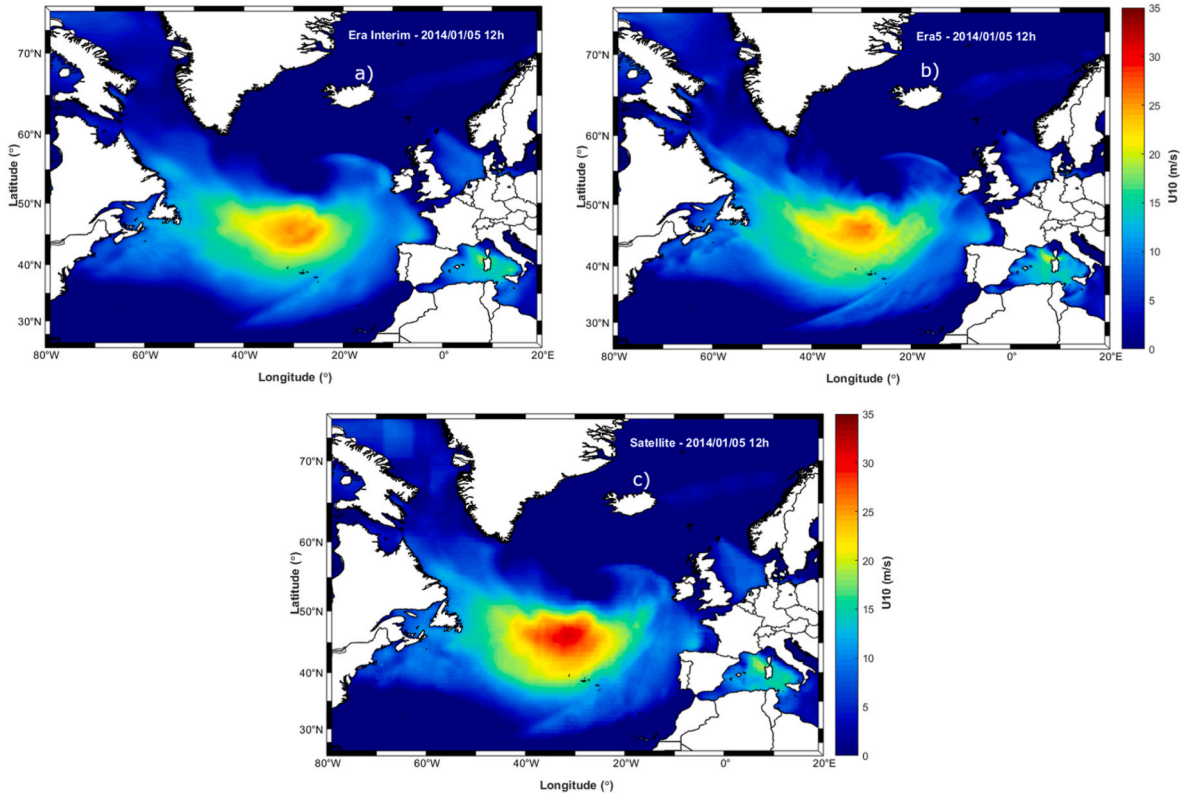

Fig. 8. U_{10} scalar fields in the North Atlantic area for the 5th of January 2014 at 12h, from ERA-Interim (a), ERA5 (b) and Scatterometer (c).

horizontal resolution (31 km grid spacing compared to 79 km for ERA-Interim), and several other innovative features. More detailed descriptions of the ECMWF reanalysis can be found in (Hersbach et al., 2019).

An overview of the main characteristics of ERA5 and a comparison with ERA-Interim is presented in Table 1.

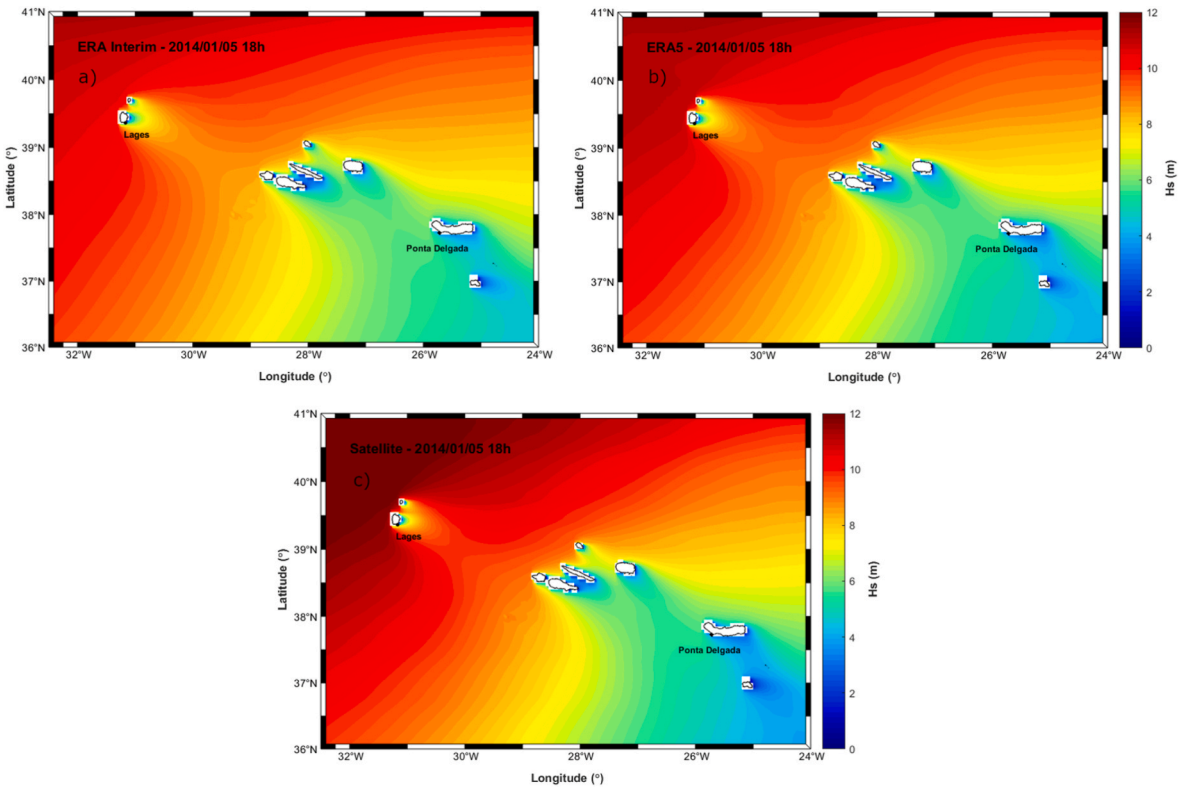

Fig. 9. Hs scalar fields in the Azores area for 5th of January 2014 at 12h, simulated with ERA-Interim (a), ERA5 (b) and Scatterometer (c) wind fields.

2.3. Remotely sensed data

The remotely sensed data used in this study, referred to here as satellite wind speed and direction, is mostly derived from scatterometer wind retrievals in combination with radiometer observations. The data and the associated methods are described in various papers (Bentamy et al., 2019; Desbiolles et al., 2017).

During the study period 2010–2014, the main sources of remotely sensed wind data are from scatterometers onboard Metop-A (2007 – present) and Metop-B (2012 – present), named ASCAT-A and ASCAT-B. Ancillary remotely sensed data are derived from radiometers Special Sensor Microwave Imager Sounder (SSMI/S) onboard the Defense Meteorological Satellite Program (DMSP) F16 (2003 – present) and F17 (2006 – present), and from WindSat onboard Coriolis satellite (2003 – present). Scatterometer and radiometer data used in this study are of Level 2 (known as L2b product). The wind retrievals are available on the radar and radiometer ground swath of wind vector cells (WVC). Scatterometer and WindSat provide both wind speed and direction at 10m height, while SSMI/S provides only 10m wind speed. The WVC grid size varies among different wind products. ASCAT-A/B WVC is 12.5 km × 12.5 km, while SSMI/S WVC is 25 km × 25 km.

Scatterometer beams measure the normalized radar cross-section (NRCS), also known as backscatter coefficient (σ^0), from the wind-roughened sea surface, which is mainly a function of wind condition (speed and direction). The σ^0 data represents a dimensionless property of the surface, describing the ratio of the effective echoing area per unit area illuminated. Scatterometer wind retrievals are obtained from σ^0 measurements through an inversion procedure based on the use of Geophysical Model Functions (GMF). Scatterometer wind retrievals provide swaths of 2 × 600 km. The links shown in Table 2 provide technical details related to scatterometer wind processing. References Desbiolles et al. (2017) and Bentamy et al. (2016) provide results related to the accuracy of scatterometer wind retrievals.

The ancillary remotely sensed wind data used in this study are retrieved from the special sensor microwave imager (SSM/I) and sounder (SSMI/S) brightness temperature measurements (TB). Only surface wind speed at 10m height can be derived from SSMI and SSMI/S TB based on the use of an empirical model fitting the relationship between surface wind speed and TB through the radiative transfer equation (RTE). They are provided by a remote sensing system (RSS) (Wentz, 2013). SSM/I and SSMI/S wind data are available over a swath of 1400 km width at a wind cell of 0.25° in latitude and longitude over global oceans.

The scatterometer retrieval in combination with radiometer wind observations, and with the ECMWF re-analysis model ERA-Interim (Simmons et al., 2006), is used for determining regular in space and time surface wind analyses (Desbiolles et al., 2017). The latter is available at synoptic times (00h:00, 06h:00, 12h:00, and 18h:00 UTC), over the global oceans with a spatial resolution of 0.25° × 0.25°.

Regarding the study topic, it is of interest to determine statistics aiming at the characterization of the satellite wind speed and direction analysis accuracy at regional (North Atlantic) and local (Azores and Madeira) scales. The most reliable method aiming at the determination of satellite wind accuracy is to perform comprehensive comparisons to buoy wind speeds and directions. For this study, the satellite wind accuracy is determined through comparisons with available buoys moored in the northeast of the Atlantic Ocean (Fig. 1).

Buoy measurements are available as hourly data. Each buoy valid wind measurements available within 3 h of synoptic times (00h:00, 06h:00, 12h:00, 18h:00 UTC), are 6-hourly averaged. For each synoptic time, available and valid 6-hourly buoy and satellite winds are spatially collocated with a difference of 12.5 km in WVC spatial separation. The statistical parameters aiming at the characterization of the comparison between buoy and satellite are estimated from the collocated data occurring along the study period (2010–2015).

"The accuracy of wind retrievals is evaluated by comparing in situ buoy measurements with quasi-simultaneous scatterometer data. The satellite-buoy data pairs collocated in space and time. The spatial limit for collocation is set based on WVC size of particular satellite wind product, which is 25 km for ERS-2 ASPS2.0, ASCAT, and QuikSCAT and

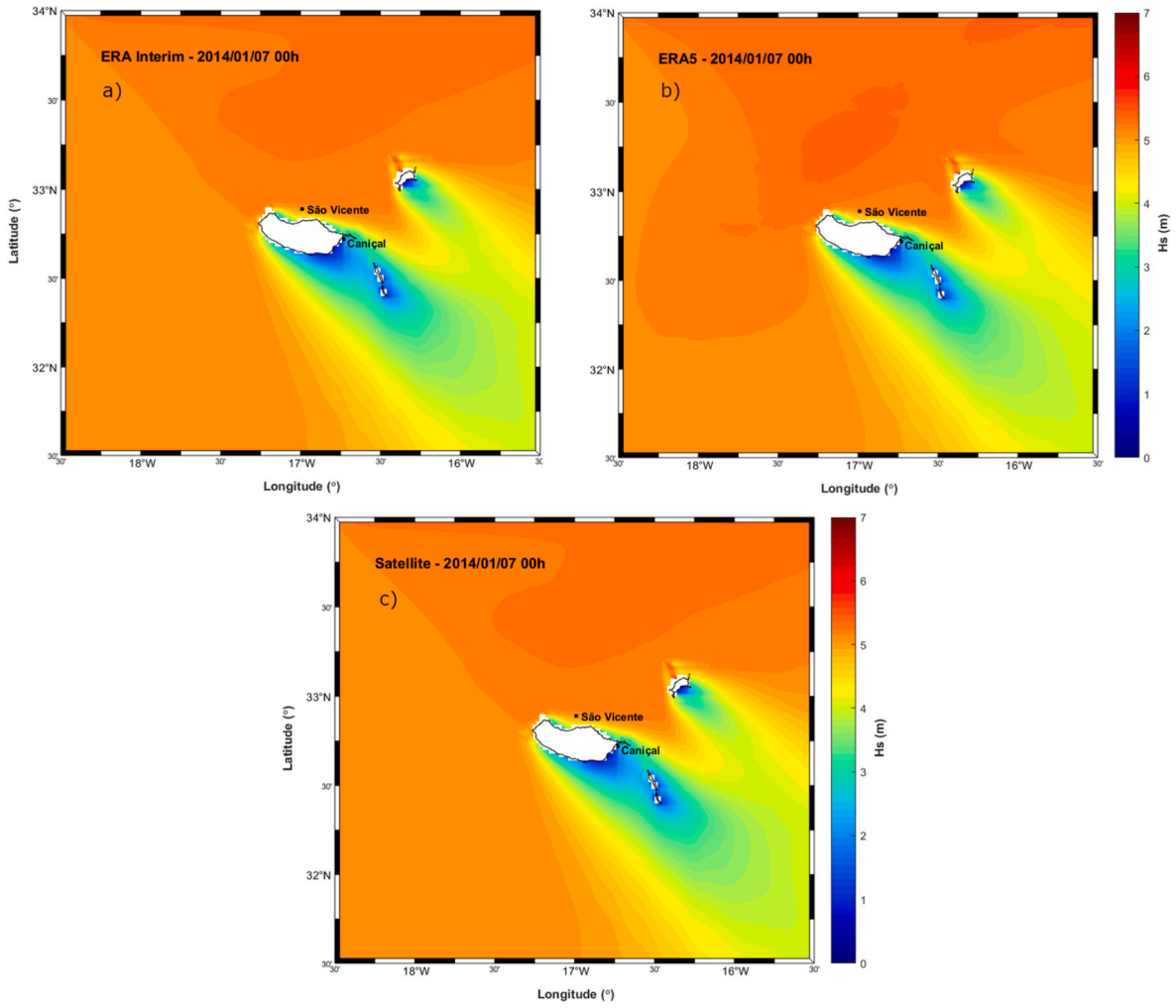

Fig. 10. Hs scalar fields in the Madeira area for 7th of January 2014 at 00h, simulated with ERA-Interim (a), ERA5 (b) and Scatterometer (c) wind fields.

Table 7
Grid points *Hs* values for the extreme event case, on the 5th of January 2014 at 12h for the Azores and the 7th of January 2014 at 00h for Madeira.

	Hs(m)			
	Lat/Lon	ERA-5	ERA-Interim	Scatterometer
Azores	**40.5°N/25°W**	9.63	9.60	9.61
	40.5°N/32°W	11.20	11.00	12.40
	39°N/30°W	9.18	8.74	9.81
	38.5°N/25°W	7.39	7.48	7.23
	37.5°N/27.7°W	6.80	6.80	6.81
	36.5°N/32°W	9.78	9.65	9.87
Madeira	**33.86°N/16°W**	5.35	5.34	5.43
	33.10°N/16.38°W	5.64	5.61	5.71
	33°N/17.5°W	5.29	5.15	5.28
	32.44°N/16.60°W	2.92	2.81	3.07
	32°N/18°W	5.12	5.10	5.13
	31.80°N/16.88°W	4.96	4.96	4.97

increases to 50 km for ERS-1 and ERS-2 WNF. To assess this hypothesis from available moorings and estimate related errors, all buoy pairs located within 50 km are selected.

In summary, no systematic bias is found between the buoy and satellite wind speeds and directions. The associated root mean square difference (RMSD) does not exceed 1.20 m/s and 20°, for wind speed and direction, respectively. The wind speed scalar correlation and wind direction vector correlation are 0.94 and 1.80, respectively.

3. Hindcast system description

3.1. Theoretical formulations

WAVEWATCH III (WWIII) is a full-spectral third-generation wind-wave model, developed by the Marine Modeling and Analysis Branch (MMAB), of the Environmental Center (EMC), of the National Centers for Environmental Prediction (NCEP) (Tolman, 2009). SWAN is also a third-generation spectral wave model developed at Delft University of Technology (Booij et al., 1999). The particularity of third-generation spectral phase-average wave models is the ability to solve the non-linear interactions of the waves using the Eulerian approach to solve the equation for the wave spectrum, which is given by:

$$\frac{DN}{Dt} = \frac{S}{\sigma} \tag{1}$$

where N represents the wave action density spectrum, S the general sources and sinks and σ the relative frequency.

The spectrum that is considered in most of the present wave models is the action density spectrum (*N*), rather than the energy density spectrum since in the presence of currents action density is conserved whereas energy density is not (Whitham, 1965).

The equation (1) is a balance in spectral energy that describes the evolution of the wave spectrum in time, geographical and spectral spaces given by:

$$\frac{\partial N}{\partial t}+\nabla_x .(\dot{x}N)+\frac{\partial}{\partial k}(\dot{k}N)+\frac{\partial}{\partial \theta}(\dot{\theta}N)=\frac{S}{\sigma} \tag{2}$$

where:

$$\dot{x}=c_g+U \tag{3}$$

$$\dot{k}=-\frac{\partial \sigma}{\partial d}\frac{\partial d}{\partial s}-k\frac{\partial U}{\partial s} \tag{4}$$

$$\dot{\theta}=-\frac{1}{k}\left[\frac{\partial \sigma}{\partial d}\frac{\partial d}{\partial m}-k\frac{\partial U}{\partial m}\right] \tag{5}$$

c_g is the group velocity of wave energy in *x, y* spatial space, U is the mean current velocity, d is the water depth, σ is the relative frequency, k is the wave number, s and m are the space coordinates of wave propagation direction θ.

The S from the right-hand side of the action balance equation represents the source terms, defined as

$$S=S_{ln}+S_{in}+S_{nl}+S_{ds}+S_{bot}+S_{db}+S_{tr}+S_{sc}+S_{xx} \tag{6}$$

For deep water, the following terms can be considered for *S*: *Snl* is a nonlinear interaction wind wave, *Sin* is the wind wave interaction and *Sds* is a dissipation term. For model initialization, *Sln* should also be considered. In shallow waters, further processes must be considered, such as the wave bottom interaction (*Sbot*), in extremely shallow water, depth-induced breaking (*Sdb*) and triad wave-wave interactions (*Str*).

SWAN is suited for intermediate and shallow water processes by including additional source terms for triad wave-wave interactions and depth-induced wave breaking as well as the JONSWAP parameterization for dissipation due to bottom friction (Hasselmann et al., 1973). In addition, SWAN accounts for some effects of diffraction by including an additional term derived from the mild slope equation (Holthuijsen et al., 2003). The mild-slope equation describes the variations of wave height when waves propagate through varying depths with the combined effects of diffraction and refraction. In terms of efficiency, WWIII tends to be more applicable in deep waters, on global scales, while SWAN tends to be more effective in shallow waters, on regional scales.

3.2. Model input and boundary conditions

For each hindcast, spectral data from WWIII, provided by the Ifremer IOWAGA (Integrated Ocean WAves for Geophysical and other Applications) project (Ardhuin and Accensi, 2013), with a time resolution of 3h (Table 3), are used as boundary conditions for the SWAN model, to study the evolution of the waves in the area of the Azores and Madeira Islands.

Each wind input field used has a time resolution of 6 h, provided over a spatial grid of 0.25°x0.25° resolution. The bathymetry used in the SWAN model is from GEBCO (General Bathymetric Chart of the Ocean), Figs. 2 and 3, and its original resolution is interpolated as presented in Table 4. To optimize the computational time consumption, the grid of the Azores area, which is a larger area than Madeira, was interpolated to a lower resolution.

4. Results and discussion

4.1. Validation of the results

The numerical results are compared and validated against altimeter data (both Madeira and Azores), provided by Ifremer, and buoy measurements from five wave buoys for the Azores, from CLIMAAT project (Azevedo and Gonçalo, 2005), (Table 5, Fig. 3).

The accuracy evaluation was performed using the statistics of the parameters Bias, root mean square error (RMSE), scatter index (SI) and Pearson's Correlation Coefficient (r), which are expressed by the following relationships:

$$Bias=\frac{\sum_{i=1}^{n}(X_i-Y_i)}{n} \tag{7}$$

$$RMSE=\sqrt{\frac{\sum_{i=1}^{n}(X_i-Y_i)^2}{n}} \tag{8}$$

$$SI=\frac{RMSE}{\widetilde{X}} \tag{9}$$

$$r=\frac{\sum_{i=1}^{n}(X_i-\widetilde{X})(Y_i-\widetilde{Y})}{\left(\sum_{i=1}^{n}(X_i-\widetilde{X})^2\sum_{i=1}^{n}(Y_i-\widetilde{Y})^2\right)^{1/2}} \tag{10}$$

where X_i and Y_i are the measured and simulated values, respectively.

Table 6 summarizes the results of the statistical parameters for the significant wave height (*Hs*) in the three hindcast runs against buoys data in the Azores area. All hindcast systems tend to overestimate the B1, B2 and B3 and underestimate B4 and B5. This difference in the model's performance could be due to the position of buoys, with the overestimation related to the ones more exposed to the wave regime and the underestimation with the ones more protected. Though, in general, the results show a good agreement between all the wind forcing with correlation values above 0.80, it is visible that less accurate results are found for buoys B2 and B4.

As written before, the performance of the three hindcast systems in both areas was checked using altimeter data from Ifremer. The validation was made using the Matlab toolbox ALTWAVE (Appendini et al., 2016), which matches the data between the model and the satellite in temporal (a limit of 1h30m) and spatial dimension (a limit of 0.25°). The statistics parameters were then calculated considering all the points included in the match.

Figs. 4 and 5 present the *Hs* parameter scatter diagram of the hindcast model results, for the 5 years, against the altimeter data. As can be seen, the results demonstrate a good correlation, with values above 0.80 for the Azores islands and 0.90 for Madeira Island. The overestimation for all the wind reanalysis in both locations is also visible.

For the locations of two buoys in each area, direct comparisons of the Hs time series results between the three wave hindcasts systems were made for 2 months (January and February of 2014), strategically chosen to cover some storms registered in the north Atlantic. The results are illustrated in Fig. 6 (case of Azores) and Fig. 7 (case of Madeira). For the Azores, it is also included the measurements registered at the buoys. This approach not only has the purpose to see the behaviour of the different wave prediction systems and their correlation but also identifying some Hs peaks, which will be discussed later in the study.

The results show a good correlation between hindcasts. Nevertheless, it is visible that all hindcast simulations tend to underestimate B5 measurements and overestimate B3 measurements at the peaks of the Azores buoys.

4.2. Analysis of the different wind forcing sources

In this chapter, to understand the difference between the three forcing winds a field analysis is performed for an extreme event that occurred in the North Atlantic.

Between January 5th and 7th, 2014, a low-pressure system approached the Portuguese coastal areas from the Atlantic Ocean. The cyclone Hercules (also named "Christina" by the University of Berlin) affected the Portuguese islands with strong winds and waves, particularly in the Azores archipelago, located further northwest in the Atlantic than Madeira, with waves up to 12m. On the island of Madeira, waves ranged the 6–7m. Its passage left substantial destruction due to strong

winds, long-period waves and intense precipitation.

Fig. 8 shows the U_{10} scalar fields when the cyclone Hercules (5th of January 2014 at 12h) passed over the North Atlantic area, as a result of ERA-Interim, ERA5 and Satellite winds.

As can be observed, the main differences are visible in the satellite reanalysis, where the highest values for the extreme event were found ($U_{10} > 30$ m/s). The ERA-Interim and ERA5 results are relatively similar (U_{10}~25 m/s).

Ponce de León and Guedes Soares (2014, 2015a,b), describe the wave parameters under North Atlantic storms obtained from a hindcast using the WAM with CFSR (reanalysis of NOAA/NCEP) as forcing wind. On the 6th of January 2014 at 00h, in the Hércules storm, the U_{10} of CFSR presented values higher than 25 m/s (Ponce de León and Guedes Soares, 2015a), and on the 14th of February 2011 at 00h presented values of 35 m/s (44 m/s at different satellites) (Ponce de León and Guedes Soares, 2015b) and on the 9th February 2017 at 12h presented values up 35 m/s (Ponce de León and Guedes Soares, 2014). For different storms, the CFSR presents values in the same range of magnitude and is in line with the values of the forcing winds used in this work. The *Hs* values using the CFSR vary between 14m (February 2013) to values up to 20m (February 2007) in the North Atlantic. It is not possible to compare these *Hs* values directly with the ones obtained here, but for the Azores, the *Hs* values are not far from the range.

Figs. 9 and 10 show the *Hs* scalar fields obtained with the different forcing in the particular areas of the Azores (5th of January 2014 at 12h) and Madeira (7th of January 2014 at 00h). As additional information, to perform a quantitative comparison, a local *Hs* assessment was done using a few grid points around the archipelagos, which results are present in Table 7.

The *Hs* spatial distribution Figures show that for the case of the extreme event, the scatterometer forcing wind gives, in general, the highest *Hs* values, followed by Era5 and Era-Interim. This difference between the forcing winds fields is amplified in places where higher values of *Hs* are already expected, more specifically in the northwest areas, where we normally can find stronger winds. This is more evident in the Azores due to this area be more exposed to the North Atlantic storms.

From Table 7 it is possible to quantify what was written before about the *Hs* spatial distributions. The area of the Azores presents the highest values for *Hs* with the highest differences between the wind forcings. This difference, taking into account the highest and lowest values of the same point, varies between 0.01m (37.5°N/27.7°W), with Satellite having the highest value and ERA-5 together with the ERA-Interim the lowest one, and 1.40m (40.5°N/32°W), with Satellite having the highest value and ERA-Interim the lowest one. Notice that the highest difference occurred in the most northwestern point. It is also worth noting the next most northwestern point (39°N/30°W), with 1.07m of differences between Satellite (highest value) and ERA-Interim (lowest value). For Madeira, the differences between the wind forcing results vary between 0.01m (31.80°N/16.88°W), related to Satellite with ERA-5 and ERA-Interim, and 0.19m (32.44°N/16.60°W), related to Satellite and ERA-Interim.

5. Conclusions

This work presents a description of the differences in the accuracy of wave conditions assessment when using different sources of wind forcing: ERA-Interim and ERA5 reanalysis, both from ECMWF, and scatterometer data. A 5-year wave hindcast system, based on the SWAN spectral wave model, has been considered and the target areas are the Portuguese islands of Azores and Madeira.

The results are validated for the Azores with buoys from the Azores and the results show that all models tend to overestimate B1, B2 and B3 and underestimate B4 and B5. The overall results show a good agreement between measurement and simulations with correlation values above 0.80.

Validations are also performed using altimeter data, for both the Azores and Madeira. The results showed a good correlation with an overestimation for all the wind forcings.

To understand the difference between the three forcing winds systems a field analysis is carried out for an extreme event that occurred in the North Atlantic. This work showed that the *Hs* outputs of the SWAN model forced by scatterometer winds present the highest values for the extreme event, followed by Era5 and Era-Interim. This difference between the forcing winds is more visible in the Azores, as this area is more exposed to the North Atlantic storms.

Finally, the results show that under extreme conditions all hindcast systems tend to underestimate the *Hs* peaks.

CRediT authorship contribution statement

Dina Silva: Methodology, Formal analysis, Visualization, Writing – original draft. **Marta Gonçalves:** Methodology, Formal analysis, Visualization, Writing – original draft. **Abderrahim Bentamy:** Formal analysis, Writing – original draft. **C. Guedes Soares:** Writing – review & editing, Supervision.

Declaration of competing interest

The authors declare that they have no known competing financial interests or personal relationships that could have appeared to influence the work reported in this paper.

Data availability

No data was used for the research described in the article.

Acknowledgements

This work was conducted within the ARCWIND project–Adaptation and implementation of floating wind energy conversion technology for the Atlantic region (EAPA 344/2016), which is co-financed by the European Regional Development Fund through the Interreg Atlantic Area Programme. This work contributes to the Strategic Research Plan of the Centre for Marine Technology and Ocean Engineering (CENTEC), which is financed by the Portuguese Foundation for Science and Technology (Fundação para a Ciência e Tecnologia - FCT) under contract UIDB/UIDP/00134/2020. The second author has been financed by FCT under the grant SFRH/BD/149858/2019. The authors are grateful to E.B. Azevedo and F. V. Reis for having made available the wave buoy data collected since 2005 by the project CLIMAAT (MAC/2.3/A3) and now obtained and processed under the framework of the ECOMARPORT project (MAC/1.1B/081).

References

Appendini, C.M., Camacho-Magaña, V., Breña-Naranjo, J.A., 2016. Altwave: toolbox for use of satellite L2P altimeter data for wave model validation. Adv. Space Res. 57, 1426–1439. https://doi.org/10.1016/j.asr.2015.12.015.

Ardhuin, F., Accensi, M., 2013. IOWAGA - WWIII - HINDCAST - North East Atlantic Grid - CFSR. https://sextant.ifremer.fr/record/f7458830-9357-4b81-8181-5492544d0a97/.

Azevedo, E.B., Gonçalo, V., 2005. O Projecto CLIMAAT e o seu Contributo para a Monotorização e Caracterização da Agitação Marítima no Arquipélago dos Açores - 4ªs Jornadas Portuguesas de Engenharia Costeira e Portuária, Angra do Heroísmo, 20 e 21 de Outubro de 2005.

Bentamy, A., Hajji, H., Guedes Soares, C., 2002. Remotely sensed wind, wave, and sea level for European sea climatology. In: International Conference on Offshore Mechanics and Arctic Engineering, vol. 36126, pp. 717–723. Paper OMAE2002-28625.

Bentamy, A., Croize-Fillon, D., Perigaud, C., 2008. Characterization of ASCAT measurements based on buoy and QuikSCAT wind vector observations. Ocean Sci. 4, 265–274. https://doi.org/10.5194/os-4-265-2008.

Bentamy, A., Croize-Fillon, D., 2014. Spatial and temporal characteristics of wind and wind power off the coasts of Brittany. Renew. Energy 66, 670–679. https://doi.org/10.1016/j.renene.2014.01.012.

Bentamy, A., Grodsky, S.A., Elyouncha, A., Chapron, B., Desbiolle, F., 2016. Homogenization of scatterometer wind retrievals. Int. J. Climatol. 37, 870–889. https://doi.org/10.1002/joc.4746.

Bentamy, A., Mouche, A., Grouazel, A., Moujane, A., Mohamed, A.A., 2019. Using sentinel-1A SAR wind retrievals for enhancing scatterometer and radiometer regional wind analyses. Int. J. Rem. Sens. 40 (3), 1120–1147. https://doi.org/10.1080/01431161.2018.1524174.

Booij, N., Ris, R.C., Holthuijsen, L.H., 1999. A third generation wave model for coastal regions. Part 1: model description and validation. J. Geophys. Res. 104, 7649–7666. Paper number: 0148-0227/99/98JC-02622$09.00.

Campos, R.M., Guedes Soares, C., 2016a. Comparison of HIPOCAS and ERA wind and wave reanalyses in the north Atlantic Ocean. Ocean Eng. 112, 320–334. https://doi.org/10.1016/j.oceaneng.2015.12.028.

Campos, R.M., Guedes Soares, C., 2016b. Comparison and assessment of three wave hindcasts in the North Atlantic Ocean. J. Operation. Oceanograph. 9, 26–44. https://doi.org/10.1080/1755876X.2016.1200249.

Campos, R.M., Guedes Soares, C., 2017. Assessment of three wind reanalysis in the north Atlantic Ocean. J. Operation. Oceanograph. 10 (1), 30–44. https://doi.org/10.1080/1755876X.2016.1253328.

Campos, R.M., D'Agostini, A., França, B.R.L., Damião, A.L.A., Guedes Soares, C., 2022. Implementation of a multi-grid operational wave forecast in the South Atlantic Ocean. Ocean Eng. 243, 110173 https://doi.org/10.1016/j.oceaneng.2021.110173.

Cavaleri, L., Bertotti, L., 2006. The improvement of modelled wind and wave fields with increasing resolution. Ocean Eng. 33, 553–565. https://doi.org/10.1016/j.oceaneng.2005.07.004.

Cavaleri, L., Alves, J.H., Ardhuin, F., Babanin, A., Banner, M., Belibassakis, K., WISE Group, 2007. Wave modelling–the state of the art. Prog. Oceanogr. 75 (4), 603–674. https://doi.org/10.1016/j.pocean.2007.05.005.

Dee, D.P., Uppala, S.M., Simmons, A.J., Berrisford, P., Poli, P., Kobayashi, S., Andrae, U., Balmaseda, M.A., Balsamo, G., Bauer, P., et al., 2011. The ERA-Interim reanalysis: configuration and performance of the data assimilation system. Quart. J. Meteorol. Soc. 137, 553–597. https://doi.org/10.1002/qj.828.

Desbiolles, F., Bentamy, A., Blanke, B., Roy, C., Mestas-Nunez, A., Grodsky, S.A., Herbette, S., Cambon, G., Maes, C., 2017. Two decades [1992-2012] of surface wind analyses based on satellite scatterometer observations. J. Mar. Syst. 168, 38–56. https://doi.org/10.1016/j.jmarsys.2017.01.003.

Gonçalves, M., Martinho, P., Guedes Soares, C., 2020. Wave energy assessment based on a 33-year hindcast for the Canary Islands. Renew. Energy 152, 259–269. https://doi.org/10.1016/J.RENENE.2020.01.011.

Gonçalves, M., Guedes Soares, C., 2021a. In: Guedes Soares, C. (Ed.), Assessment of the Wave Energy Resource in the Azores Coastal Area", Developments in Renewable Energies Offshore. Taylor and Francis, London, UK, pp. 26–33.

Gonçalves, M., Guedes Soares, C., 2021b. Assessment of the wave conditions in the Azores coastal area. In: Guedes Soares, C., Santos, T.A. (Eds.), Developments in Maritime Technology and Engineering, vol. 2. Taylor and Francis, London, UK, pp. 569–576.

Guedes Soares, C., 2008. Hindcast of dynamic processes of the ocean and coastal areas of Europe. Coast. Eng. 55, 825–826. https://doi.org/10.1016/j.coastaleng.2008.02.007.

Guedes Soares, C., Rusu, L., Bernardino, M., Pilar, P., 2011. An operational forecasting system for the Portuguese continental coastal area. J. Operation. Oceanograph. 4 (2), 17–27.

Hasselmann, K., Barnett, T.P., Bouws, E., Carlson, H., Cartwright, D.E., Enke, K., et al., 1973. Measurements of Wind-Wave Growth and Swell Decay during the Joint North Sea Wave Project (JONSWAP). Deutsche Hydrographische Zeitscheift, p. 95. A8(12).

Hersbach, H., Dee, D., 2016. ERA5 reanalysis is in production. ECMWF Newslett. 147, 7. https://www.ecmwf.int/en/newsletter/147/news/ERA5-reanalysis-production.

Hersbach, H., Bell, B., Berrisford, P., Horányi, A., Muñoz-Sabater, J., Nicolas, P., Radu, R., Schepers, D., Simmons, A., Soci, C., Dee, D., 2019. ECMWF Global Reanalysis: hello ERA5, goodbye ERA-Interim. ECMWF Newslett. 159 https://doi.org/10.21957/vf291hehd7 (in press).

Holthuijsen, L.H., Booji, N., Bertotti, L., 1996. The propagation of wind errors through Ocean WAve hindcasts. J. Offshore Mech. Arctic Eng. 118, 184–189. https://doi.org/10.1115/1.2828832.

Holthuijsen, L.H., Herman, A., Booij, N., 2003. Phase-coupled refraction and diffraction for spectral wave models. Coast. Eng. 49, 291–305. https://doi.org/10.1016/S0378-3839(03)00065-6.

Jiang, D., Zhuang, D., Huang, Y., Wang, J., Fu, J., 2013. Evaluating the spatio-temporal variation of China's offshore wind resources based on remotely sensed wind field data. Renew. Sustain. Energy Rev. 24, 142–148. https://doi.org/10.1016/j.rser.2013.03.058.

Lavidas, G., Venugopal, E., Friedrich, D., 2017. Sensitivity of a numerical wave model on wind reanalysis datasets. Dynam. Atmos. Oceans 77, 1–16. https://doi.org/10.1016/j.dynatmoce.2016.10.007.

Mulligan, R.P., Perrie, W., Toulany, B., Smith, P.C., Hay, A.E., Bowen, A.J., 2011. Performance of nowcast and forecast wave models for Lunenburg Bay, Nova Scotia. Atmos.-Ocean 49 (1), 1–7. https://doi.org/10.1080/07055900.2011.558468.

Ponce de León, S., Guedes Soares, C., 2005. On the sheltering effect of islands in ocean wave modelling. J. Geophys. Res. 110, C09020.

Ponce de León, S., Guedes Soares, C., 2008. Sensitivity of wave model predictions to wind fields in the Western Mediterranean sea. Coast. Eng. 55, 920–929. https://doi.org/10.1016/j.coastaleng.2008.02.023.

Ponce de Leon, S., Guedes Soares, C., 2010. The sheltering effect of the Balearic Islands in the hindcast wave field. Ocean Eng. 37 (7), 603–610.

Ponce de Leon, S., Guedes Soares, C., 2014. Extreme wave parameters under North Atlantic extratropical cyclones. Ocean Model. 81, 78–88. https://doi.org/10.1016/j.ocemod.2014.07.005.

Ponce de Leon, S., Guedes Soares, C., 2015a. Hindcast of the Hércules winter storm in the north Atlantic. Nat. Hazards 78, 1883–1897. https://doi.org/10.1007/s11069-015-1806-7.

Ponce de Leon, S., Guedes Soares, C., 2015b. Hindcast of extreme sea states in North Atlantic extratropical storms. Ocean Dynam. 65, 241–254. https://doi.org/10.1007/s10236-014-0794-6.

Ricciardulli, L., Manaster, A., 2021. Intercalibration of ASCAT scatterometer winds from MetOp-A,-B, and -C, for a stable climate data record. Rem. Sens. 13, 3678. https://doi.org/10.3390/rs13183678.

Roland, A., Ardhuin, F., 2014. On the developments of spectral wave models: numerics and parameterizations for the coastal ocean. Ocean Dynam. 64 (6), 833–846.

Rusu, E., Pilar, P., Guedes Soares, C., 2008. Evaluation of the wave conditions in Madeira archipelago with spectral models. Ocean Eng. 35 (13), 1357–1371. https://doi.org/10.1016/j.oceaneng.2008.05.007.

Rusu, L., Pilar, P., Guedes Soares, C., 2008. Hindcast of the wave conditions along the west Iberian coast. Coast. Eng. 55, 906–919.

Rusu, L., Guedes Soares, C., 2012. Wave energy assessments in the Azores islands. Renew. Energy 45, 183–196. https://doi.org/10.1016/j.renene.2012.02.027.

Rusu, L., Goncalves, M., Guedes Soares, C., 2018. Prediction of storm conditions using wind data from the ECMWF and NCEP reanalysis. In: Guedes Soares, C., Teixeira, A. P. (Eds.), Maritime Transportation and Harvesting of Sea Resources. Taylor & Francis Group, London, UK, pp. 1111–1117.

Saha, S., Moorthi, S., Pan, H., Wu, X., Wang, J., Nadiga, S., Tripp, P., Kistler, R., Wollen, J., Behringer, D., et al., 2010. The NCEP climate forecast system reanalysis. Bull. Am. Meteorol. Soc. 91, 1015–1057. https://doi.org/10.1175/2010BAMS3001.1.

Silva, D., Martinho, P., Guedes Soares, C., 2018. Wave energy distribution along the Portuguese continental coast based on a thirty-three years hindcast. Renew. Energy 127 (4), 1067–1075.

Silva, D., Guedes Soares, C., 2021a. Assessment of the wave power resource at Madeira archipelago with SWAN model. In: Guedes Soares, C. (Ed.), Developments in Renewable Energies Offshore. Taylor and Francis, London, UK, pp. 45–54.

Silva, D., Guedes Soares, C., 2021b. Validation with satellite data of SWAN model for wave conditions at the Madeira archipelago. In: Guedes Soares, C., Santos, T.A. (Eds.), Developments in Maritime Technology and Engineering, vol. 2. Taylor and Francis, London, UK, pp. 665–672.

Simmons, A., Uppala, S., Dee, D., Kobayashi, S., 2006. ERA-Interim: New ECMWF reanalysis products from 1989 onwards. ECMWF Newslett. 110, 26–35. https://doi.org/10.21957/pocnex23c6.

Stopa, J.E., Cheung, K.F., 2014. Intercomparison of wind and wave data from the ECMWF reanalysis Interim and the NCEP climate forecast system reanalysis. Ocean Model. 75, 65–83. https://doi.org/10.1016/j.ocemod.2013.12.006.

Stopa, J.E., Ardhuin, F., Girard-Ardhuin, F., 2016. Wave climate in the Arctic 1992–2014: Seasonality and trends. Cryosphere 10 (4), 1605–1629.

Sudha, A.K., Prasada Rao, C.V.K., 2013. Comparison of Oceansat-2 scatterometer winds with buoy observations over the Indian ocean and the Pacific ocean. Rem. Sens. Lett. 4, 171–179. https://doi.org/10.1080/2150704X.2012.713140.

Teixeira, J.C., Abreu, M.P., Guedes Soares, C., 1995. Uncertainty of Ocean WAve hindcasts due to wind modelling. J. Offshore Mech. Arctic Eng. 117, 294–297. https://doi.org/10.1115/1.2827237.

Tolman, H.L., 1991. A third-generation model for wind waves on slowly varying, unsteady, and inhomogeneous depths and currents. J. Phys. Oceanogr. 21, 782–797. https://doi.org/10.1175/1520-0485(1991)021<0782:ATGMFW>2.0.CO;2.

Tolman, H.L., 2009. User Manual and System Documentation of WAVEWATCH III Version 3.14, vol. 276. NOAA/NWS/NCEP/MMAB Technical Note, p. 194.

Verhoef, A., Vogelzang, J., Verspeek, J., Stoffelen, A., 2016. Long-term scatterometer wind climate data records. IEEE J. Sel. Top. Appl. Earth Obs. Rem. Sens. 1–9. https://doi.org/10.1109/JSTARS.2016.2615873.

Verspeek, J., Stoffelen, A., Portabella, M., Bonekamp, H., Anderson, C., Saldana, J.F., 2010. Validation and calibration of ASCAT using CMOD5.n. IEEE Trans. Geosci. Remote Sens. 48, 386–395.

WAMDI Group, 1988. The WAM model-a third generation ocean wave prediction model. J. Phys. Oceanogr. 18, 1755–1810. https://doi.org/10.1175/15200485(1988)018<1775:TWMTGO>2.0.CO;2.

Wentz, F.J., 2013. SSM/I Version-7 Calibration Report. Remote Sensing Systems, Santa Rosa, CA, p. 46pp report number 011012.

Whitham, G.B., 1965. A general approach to linear and non-linear dispersive waves using a Lagrangian. J. Fluid Mech. 22 (2), 273–283.